New insights into microbially induced sedimentary structures in alkaline hypersaline El Beida Lake, Wadi El Natrun, Egypt

Amany G. Taher & Ali Abdel-Motelib

Geo-Marine Letters
An International Journal of Marine Geology

ISSN 0276-0460
Volume 35
Number 5

Geo-Mar Lett (2015) 35:341-353
DOI 10.1007/s00367-015-0411-9

Springer

Geo-Mar Lett (2015) 35:341–353
DOI 10.1007/s00367-015-0411-9

ORIGINAL

New insights into microbially induced sedimentary structures in alkaline hypersaline El Beida Lake, Wadi El Natrun, Egypt

Amany G. Taher[1] · **Ali Abdel-Motelib**[1]

Received: 23 March 2015 / Accepted: 19 May 2015 / Published online: 29 May 2015

Abstract Microbially induced sedimentary structures (MISS) were studied in detail in the alkaline hypersaline El Beida Lake of Wadi El Natrun in the western desert sector of Egypt, based on field observations and sampling performed in 2013 and 2014. Geomorphologically, the lake can be subdivided into three zones, each with characteristic sedimentary and biosedimentary structures. The marginal elevated zone that borders the lake is characterized by thick blocky crusts devoid of microbial mats. The middle–lower supratidal zone has luxuriant microbial mats associated with knotty surfaces, mat cracks and wrinkle structures. A zone of ephemeral shallow pools and channels is characterized by reticulate surfaces, pinnacle mats, sieve-like surfaces, gas domes and mat chips. In the microbial mats, authigenic minerals include thenardite Na_2SO_4, trona $Na_3(CO_3)(HCO_3)•2H_2O$ and halite NaCl. Scanning electron microscopy (SEM) analyses revealed that the minerals are closely associated with the MISS, suggesting some influence of microorganisms on mineral precipitation. Complex interactions between regional hydrological cycles and diagenetic processes imply low preservation potential. MISS signatures of such saline lakes can serve as key analogues for interpreting the geologic record.

Introduction

Microbial mats are advanced biofilm stages forming laminae on bedding surfaces where they reflect gaps in sedimentation or, in other terms, time periods of growth, biomass condensation and biological succession (Gerdes 2010). The most common expression of photosynthesis in rocks is fossilized photosynthetic microbial mats resulting from interactions with sediments, environmental conditions and geological processes at a wide range of scales (Bouougri et al. 2012). Microbial mats flourish in various settings including continental and deep sea basins, peritidal environments (e.g. Gerdes and Krumbein 1987), salt works (e.g. Taher 2014a; Aref et al. 2014), cold seep sediments (e.g. Grünke et al. 2012), hydrothermal vents (e.g. Jeanthon 2000) and methane-derived deposits (e.g. Wrede et al. 2013). Commonly, they are constituted by benthic microbial communities usually dominated by photosynthetic prokaryotes, particularly cyanobacteria, and occasionally by eukaryotic microalgae such as diatoms. Cyanobacteria are the only oxygenic phototrophs known to have existed from before 2 Ga up to the present day (Knoll et al. 2012). Development of microbial mats requires sufficiently low sedimentation rates that accommodate vertical displacement of photoautotrophic microorganisms towards the sediment surface to obtain optimum sunlight (Gerdes et al. 2000).

Microbial mats secrete extracellular polymeric substances (EPS) that enable adherence to the substratum (Decho 2000), in the form of sticky coatings on individual sedimentary particles (Noffke 2010). EPS forms the matrix of the mat in which the microorganisms are embedded (Yallop et al. 1994), and it plays a role in binding essential metals, as well as protecting the microbes from, for example, desiccation (e.g. Taher et al. 1994; Decho 2000; Noffke 2010). Microbial mats and biofilms have significant impacts on the response of sediments to the hydraulic dynamics of waves and currents (e.g. Noffke and Krumbein 1999; Gerdes et al. 2000; Hagadorn and McDowell 2012; Taher and Abdel Motelib 2014; Cuadrado et al. 2014).

The activities of benthic prokaryotes in response to sediment dynamics form characteristic structures named microbially induced sedimentary structures (MISS; Noffke 2010). Their formation has been well studied in modern tidal flats where benthic cyanobacteria are most abundant (Noffke

✉ Amany G. Taher
agtaher@yahoo.com

[1] Geology Department, Faculty of Science, Cairo University, Cairo, Egypt

et al. 1997; Noffke 1998). The wide range of microbial signatures in sediments supports recognition of biogenicity in analogous fossil patterns (Noffke 2010, 2015).

Within this context, the main goal of this investigation was a detailed study of MISS in the El Beida Lake of Wadi El Natrun in the western desert sector of Egypt. This is a unique setting comprising siliciclastic evaporitic sediments in a hypersaline alkaline environment. The findings are evaluated with regard to MISS recognition in the geologic record.

Physicochemical setting and study area

Approximately 80 km northwest of Cairo, Wadi El Natrun is an elongated depression about 60 km long and 10 km wide with its bottom situated about 23 m below sea level and 38 m below the water level of the neighbouring western (Rosetta) branch of the Nile (Fig. 1; Abd-el-Malek and Rizk 1963). This Wadi and adjacent areas have long attracted much attention focused on regional geological mapping for the purpose of oil exploration, evaluation of groundwater potential, ecosystem conservation, as well as geochemical and sediment dynamics (e.g. Shata and El-Fayoumi 1967; Abu Khadra 1973; Abu Zeid 1984; Taher 1999; Taher and Soliman 1999; Saleh 2004; Abd El Ghani et al. 2014). Quaternary deposits formed of old alluvial sands and gravels are interspersed with lake deposits laid down when the sea encroached the area and the Nile flowed through it (Phillip et al. 1975). The lake deposits and the alluvium are underlain by limestones of Pliocene, Miocene and Oligocene age.

Along the NW–SE axis of Wadi El Natrun are aligned seven large alkaline, hypersaline lakes in addition to numerous ephemeral pools, including the El Beida Lake (Fig. 1). The lakes and salt crusts lie close to the topographic chart zero contour (Abu Zeid 1984). Lake waters have extremely high salt concentrations of 91.0–393.9 g/l, and pH values of 8.5–11 (Taher 1999). Additionally, the lake waters and sediments harbour a unique prokaryotic diversity that differs from that described for similar settings in other world regions (Mesbah et al. 2007). Most lakes reach maximum levels in winter between December and March, with lowest levels in summer. Their depths range between 0.5 and 2 m, regulated by seasonal changes in influx seepage and evaporation (Mesbah et al. 2007).

Drainage is via small rills and streamlets with highly variable drainage patterns (Attia et al. 1970). The origin of the water entering the Wadi remains unclear. Pavlov (1962) suggested a radial inflow of underground waters towards the lakes, whereas Shata and El-Fayoumi (1967) argued in favour of underground flow from the Rosetta branch of the Nile, a view supported by Attia et al. (1970). By contrast, chemical and isotopic data reported by Sturchio et al. (1998) suggest the source being rainwater that occasionally infiltrates the shallow alluvial and Eocene limestone aquifers in the wider study area.

The study region has an arid climate, with low and very variable rainfall in winter, a long dry summer, high rates of evaporation, and low humidity. The main wind direction is from the northwest but the El-Khamasin wind (April–May) from the southeast is quite strong and lasts for several days, with considerable effects on precipitation and sand remobilization particularly in the south-western sector. Meteorological data recorded at local weather stations for the period 2000–2010) showed a mean annual temperature of 25.6 °C, mean annual rainfall of 2.1 mm, and mean monthly relative humidity ranging from 17% in May to 73% in December. Wind velocity varies between 11 km/h in December and January to 22 km/h in June.

This study focuses on the El Beida Lake (Quarry of Trona). Beida is a translation of the Arabic word for 'white', presumably reflecting the colour of the lake (Fig. 1b). The lake shore extends about 300 m inland and represents a typical tidal flat-like environment with a broad supratidal area. The lake is up to 2 m deep, and has hypersaline, highly alkaline, Na-CO_3-SO_4-Cl brines with a salinity of 350 g/l and pH 9.5 (Taher 1999). Predators (e.g. gastropods) are scarce due to this high salinity. By contrast, microbial films and mats can reach considerable thicknesses of 20–30 mm at the bottom and margins of pools, as well as in the lower supratidal shallows and parts of the higher lying flats flooded at irregular intervals during strong onshore winds. The lake receives a limited supply of ground water supplemented by natural springs and minor irrigation water (Abu Zeid 1984), and is marked by strong fluctuations in water level and salinity.

The surface deposits comprise aeolian sand and silt, weathered gypseous clays and decayed organic matter, reflected in the common occurrence of dark sediment patches and layers (Abu Khadra 1973). The salt deposits are particularly rich in thenardite Na_2SO_4, trona $Na_3(CO_3)(HCO_3)•2H_2O$ and halite NaCl, which form thin crusts. Halite is by far the most dominant mineral. Natron $Na_2CO_3•10H_2O$ forms crusts along the lake edges and occurs in deposits at the lake bottom.

Materials and methods

In the El Beida Lake, field observations and sampling were performed in 2013 and 2014, in each year during a winter (December–February) and a summer fieldtrip (June–September). Quantitative analyses and full documentation of the morphology of the bio-sedimentary structures were undertaken at carefully selected sites.

Petrographical and mineralogical analyses were conducted on thin sections and powdered rock material respectively. Mineralogy was determined by means of a Philips X-ray diffraction model PW/1710 with monochromator, Cu radiation (k = 1.542 Å) at 40 kV, 35 mA and scanning speed 0.02°/s. Reflection peaks were recorded between 2h = 2° and 60°, with

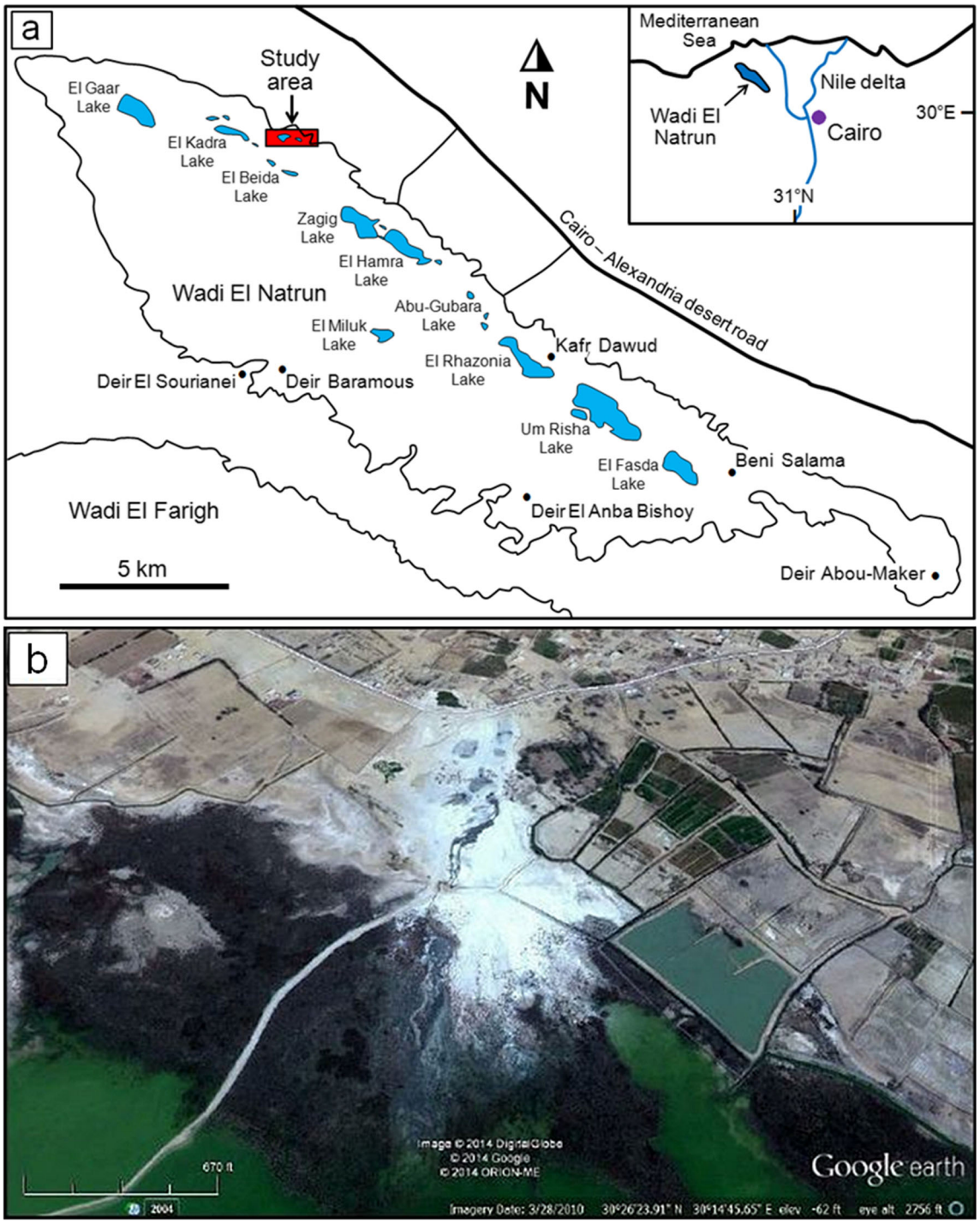

Fig. 1 **a** Location map of the study area. **b** Satellite image of the El Beida Lake (http://earth.google.com/)

corresponding spacing (d, Å) and relative intensities. The latter were compared with ICDD charts. Mineralogical samples for scanning electron microscopy (SEM) analyses were critical-point dried, gold-sputtered, and examined under an SEM Jeol JSM 35 CF.

In different zones colonized by microbial mats and biofilm-forming assemblages, samples were collected by inverting a Petri dish and pressing it into the mat. The dish was then removed, and the shallow mat core carefully lifted and placed right-side-up in the Petri dish. The samples were examined under a binocular microscope and by light microscopy. For SEM analyses, eight samples were placed in small glass tubes (diameter 0.1 cm) and fixed immediately in a 4% glutaraldehyde solution diluted with water from the sampling site.

Dewatering was in an ethanol series from 10 to 95%, followed by two treatments with absolute ethanol. Samples were then critical-point dried, gold-sputtered, and studied under the SEM.

Results

Based on topographic relief, three geomorphological zones were identified in the El Beida Lake. These comprise a marginal elevated zone I, a middle–lower supratidal zone II, and zone III characterized by ephemeral shallow pools and channels (Fig. 2).

Marginal elevated zone I

Zone I is the highest topographic zone along the shore of the lake, extending up to about 300 m inland (Fig. 2a) and only sporadically flooded during rare heavy rainfall. It is characterized by thick blocky crusts with pronounced surface relief (>0.15 m; Fig. 3a). The topographic relief, measured laterally over distances of a few tens of metres, increases with the thickness of the crusts that can reach 0.60 m associated with a surface relief of 0.40–0.50 m.

Zone I is barren of microbial mats. The sediments forming the crusts are mainly fine sand and silt hosting evaporite minerals, mostly trona with some halite. Trona crystals are prismatic in shape, vertically oriented, and up to 30 mm long. Discontinuous thin layers of white and greyish white halite, several mm to several cm thick, are precipitated in the topmost parts of the crusts. The abundance of evaporite minerals increases with proximity to the lake shore. Under the microscope, prismatic to sub-prismatic long and thin lathes of randomly oriented trona crystals with some scattered halite crystals were identified (Fig. 3b, c).

Middle–lower supratidal zone II

Low-gradient supratidal zone II is flooded sporadically during strong onshore winds, enabling initial microbial colonization and a progressive formation of a coherent network of microbial mats. This zone is characterized by highly variable morphological surface shapes of patchy distribution fluctuating over distances of a few tens of metres.

Knotty surfaces occur in the higher parts of the flats and extend to the very shallow parts of isolated pools (Fig. 3d, e). Numerous tiny, tightly spaced tufts characterize this surface of knotty appearance. They protrude up to 20 mm above the sediment surface, with diameters reaching 15 mm (Fig. 3d, e). The SEM image of Fig. 3f reveals that the tufts comprise filamentous cyanobacteria associated with EPS.

Mat cracks are characterized by distinctive convoluted patterns that are polygonal in planform (Fig. 4). They present upward-curling margins with rounded edges. Initially, the still-wetted, exposed mat sediments form uneven, somewhat lined, slightly shrunk cracks (Fig. 4a). In advanced stages particularly during summer upon long subaerial exposure, the mats loose more water. This results in further shrinkage and the formation of mat crack polygons of variable shapes and sizes with curled, upturned margins (Fig. 4b). The curled margins can be 6 to 30 mm high above a mat comprising three to five thin layers (Fig. 4c). The polygons have diameters ranging from 50 mm to 0.30 m. The spaces in between the polygons are filled with fine aeolian sand, silt, and fine argillites with salt residues.

Wrinkle structures are characterized by numerous sinuous to curved ridges up to 40 mm in size. They have round crests and hollow interiors, and are patchily distributed at the wet, cohesive, flexible mat surface (Fig. 5a). Strong wind-driven currents cause the deformation of sediment laminae otherwise stabilized by the mat, resulting in folds or wrinkles. The wrinkles are variously orientated, consistent with fluctuations in wind direction over successive days. Wrinkle patches up to 0.10 m in size (Fig. 5b) were recorded in the very hot summer season. The outlines of this type of wrinkles have a broad apex towards the lake (SW), whereas wrinkles characterized by narrow apexes were recorded towards the land. The dimensions of such structures increase towards the southwest of the lake. Slightly to highly lithified wrinkles were observed at the end of summer (August–September, Fig. 5b, c). Under the microscope, prismatic and acicular, closely packed crystals of trona were identified at the surface of organic-rich layers (Fig. 5d). Fine crystals of halite were also observed.

Zone III: pools and channels

Ephemeral shallow pools occur immediately east of the lake and show strong seasonal fluctuations in water level (Fig. 2b), in turn accompanied by significant variations in size, salinity and temperature. The surface deposits are essentially quartz grains of aeolian origin cemented by salt formed by evaporation in spring and summer. During the summer, most of these pools dry out and the benthic communities form typical drought crusts in which the microorganisms survive in a physiologically inactive form. The vegetation is patchy and characterized by, amongst others, *Juncus acutus* L., *J. rigidus* Desf., *Cyperus laevigatus* L. var. *laevigatus* and *Phragmites australis* (Cav.) Trin. ex Steud. subsp. *australis* (El Hadidi 1993; Abd El Ghani et al. 2014).

Reticulated surfaces line the bottom of the small low-lying pools as well as the channels feeding these pools, and abound where the water depth does not exceed 20 mm. They occur on the microbial mat surface and consist of intersecting horizontal linear bulges and vertical acmes (Fig. 6a, b). The linear bulges are only 2 to 3 mm high. These horizontal, thread-like microbial bodies crosscut and interconnect to produce multilateral or polygonal geometric shapes. The polygonal

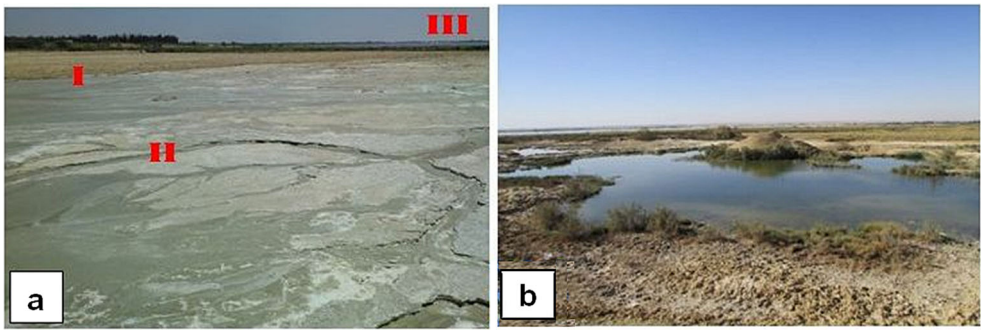

Fig. 2 Geomorphological zones of the El Beida Lake. **a** Higher marginal elevated zone (I), lower–middle supratidal zone (II) and zone of ephemeral shallow pools (III). **b** Shallow pools with patchy vegetation

shapes are mostly equidimensional (Fig. 6b), but some are elongated. Larger polygons are always associated with thicker bulges. Acmes rise above the mat surfaces at the intersections of the bulges, and vary in height from 1 to 5 mm. The SEM analyses show that filamentous cyanobacteria dominate the uppermost layers approx. 2 mm below the reticulated surfaces (Fig. 6c). Siliciclastic grains of fine sand and silt occur in the deeper layers. The underlying sediment is characterized by abundant buried organic matter (Fig. 6d).

Pinnacle mats occur in permanently water-filled shallow pools of depth not exceeding 0.10 m. The cone-like pinnacles are 10–20 mm high and 1–10 mm in diameter (Fig. 7a, b). They form large patches and commonly stand vertically; a diagonal position reflects the effect of wind direction. A cross section of the mat (Fig. 7b) shows that the pinnacles are sticky and covered with EPS. There is an underlying pink layer (<2 mm thick) consisting of phototrophic purple sulphur bacteria, in turn underlain by a thick black layer rich in organic matter. The pinnacle wall is a mixed framework of diatoms and filamentous cyanobacteria (Fig. 7c, d). EPS accumulates within depressions between individual pinnacles.

Sieve-like surfaces comprise tiny pits formed by the escape of photosynthetic gas bubbles at the thin mat–sediment

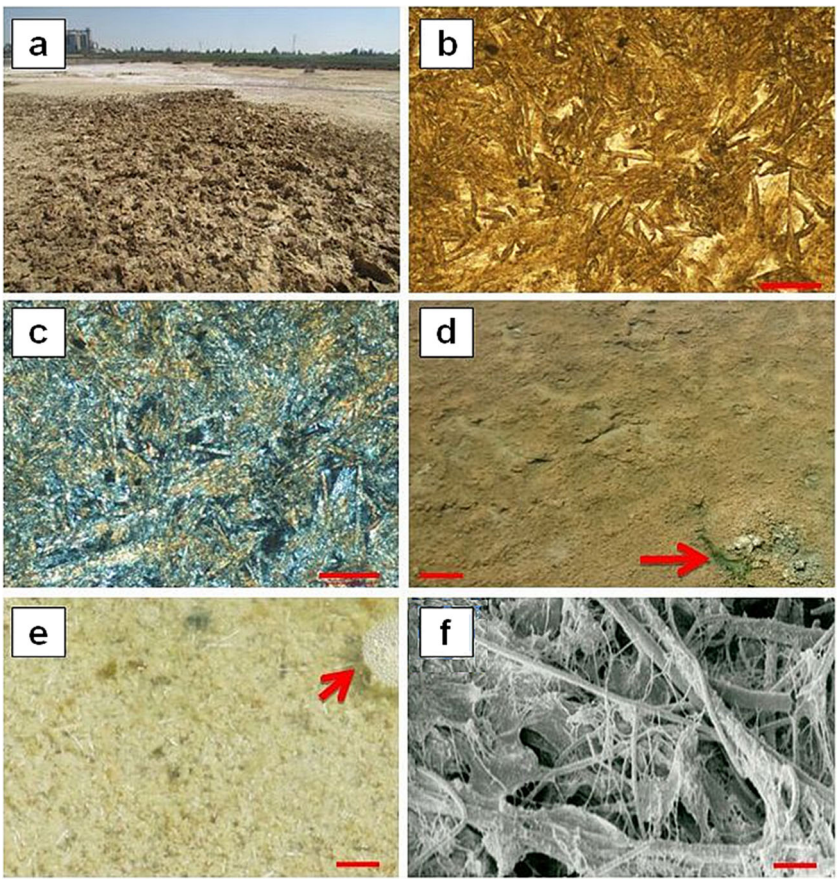

Fig. 3 **a** Blocky salt crust margin of the El Beida Lake. **b** Light microscope image of long, thin prismatic to subprismatic trona with irregularly scattered halite crystals (scale 100 μm). **c** Same image, crossed Nichols (scale 100 μm). **d** Knotty surface formed of tufts projecting through the mat surface (scale 50 mm). *Arrow* Microbial mats. **e** Closely spaced tuft cluster of filamentous cyanobacteria projecting through a surface mat under a thin veneer of water (scale 30 mm). *Arrow* Bubbles. **f** SEM image of a mat knotty surface with filamentous cyanobacteria associated with EPS (scale 5 μm)

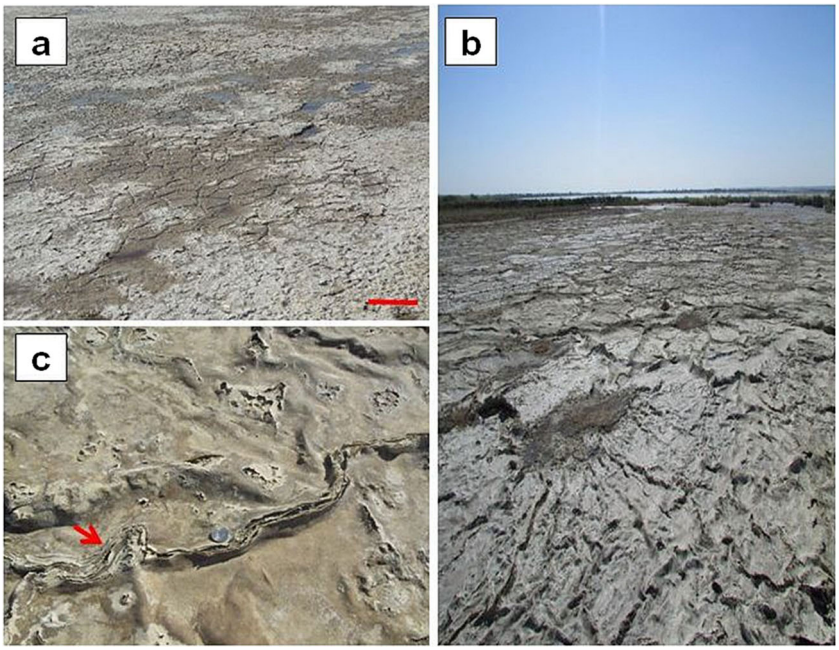

Fig. 4 Mat cracks. **a** Polygonal slightly cracked microbial mats covered by a thin veneer of water. The deeper areas in between the polygons are also wet. Scale 20 cm. **b** Mat crack polygons with upward-curled, rounded and slightly upturned margins. **c** Curled margins of mat crack polygons, showing more than one mat layer. *Arrow* Slightly upturned margin. Coin 20 mm

surface (Bose and Chafetz 2009; Fig. 8a). They are 1 to 3 mm deep with diameters reaching approx. 6 mm. Microbial mats release oxygen bubbles into the overlying shallow water layer, and these are stabilized by EPS and may merge to generate a net-like pattern. The EPS form light, circular to hexagonal, nutrient-rich rims and interstitial patches around dark hollows (Fig. 8b). During the hot season the salts crystallize, initially in the spaces between the bubbles and then inside the bubbles (Fig. 8c, d).

Gas domes form blister surfaces of protuberances with hollow cavities (Fig. 9). Gas domes were typically abundant in inundated shallow parts of pools at water depths of about 50–80 mm. They are generally 10 to 40 mm in diameter. Biofilms commonly tightly bind and envelope the domes (Fig. 9b). Dome size increases in thicker mats. Smaller domes can coalesce to form larger ones. Most domes have smooth, intact surfaces and can last several days; others have fractured crests due to escaping gases and eventually collapse, producing a

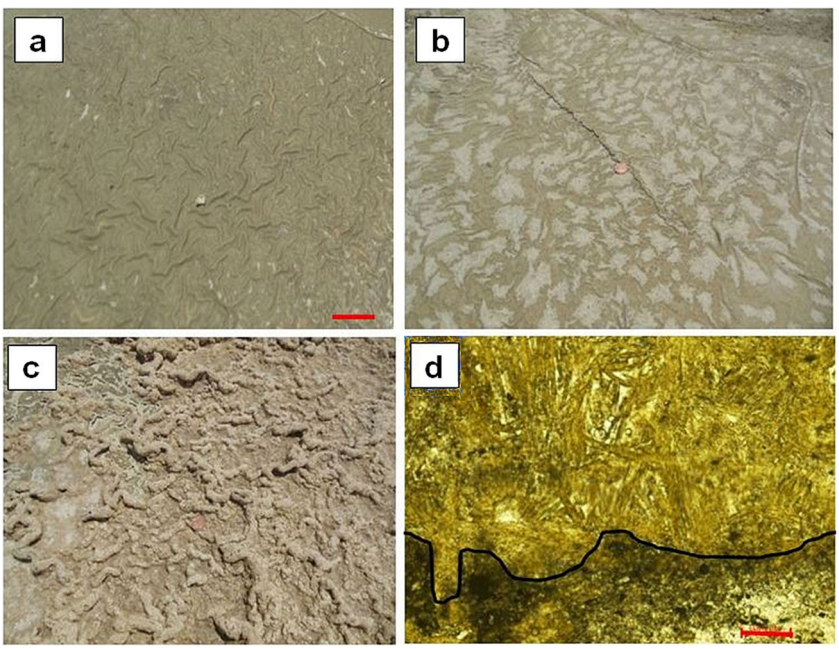

Fig. 5 Wrinkle structures. **a** Wrinkle structure of rippled appearance at mat surface (scale 30 mm). **b** Wrinkle structure of patchy appearance, slightly lithified with the substrate still wet (coin 22 mm). **c** Dry lithified wrinkle structure (coin 22 mm). **d** Crystallization of trona on the surface of organic material (darker area below *black line*; scale 100 μm)

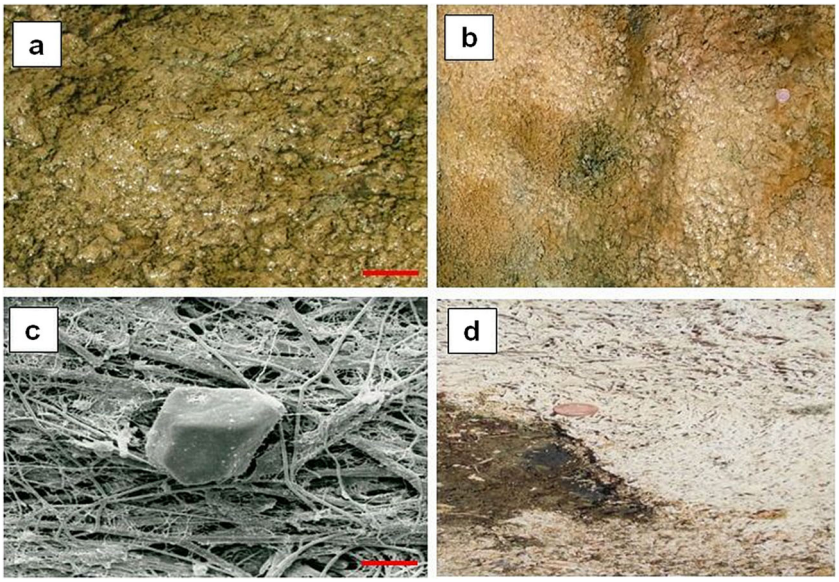

Fig. 6 Reticulated surfaces of siliciclastic sediments. **a** Reticulated surface microbial mats lining shallow supratidal pools (scale 50 mm). **b** Macroscopic surface view of a reticulated microbial mat resembling elephant skin (coin 22 mm). **c** SEM image of filamentous cyanobacteria associated with a sand grain in the uppermost few mm below the reticulated surface (scale 5 μm). **d** More elevated areas characterized by dry reticulated surface pattern (coin 22 mm). *Dark subsurface patch* Organic matter enrichment

crumpled surface (Fig. 9c). Strong gas escape was observed when scratching the surface (Fig. 9d).

Mat chips occur mainly in low-lying ponded areas and low-gradient flat areas where the mats are more frequently covered with water over longer periods of time. The mat-stabilized sediment surfaces are broken into tiny mat–sediment fragments by strong wind-driven currents (Fig. 10a). The chips appear as eroded, irregularly shaped and often with rounded to sub-rounded edges. Their size varies between about 20 and 60 mm, rarely exceeding 80 mm. Mat chips were recorded also in dry areas around the pools (Fig. 10b).

Mineral precipitation

Field observations revealed a close association between mineral precipitation and the top, oxygenated layer of the mats (Fig. 11) in the low-lying areas of zone II. In the hot season due to fast evaporation, evaporites form either as scattered crystals or as white to pink encrustations. The scattered crystals are halite, which is strongly attached to the substrate (Fig. 11a). Crystal colour ranges from grey to clear white to transparent. Crystals with high volumes of fluid inclusions have a cloudy appearance. The crusts growing at the surface reach maximum depths of about 50 mm, and comprise sphere-

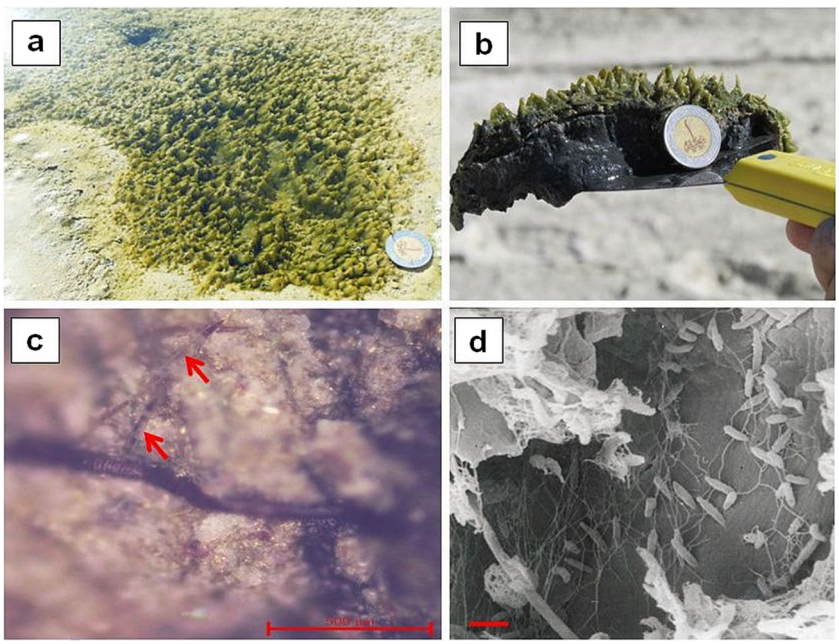

Fig. 7 Pinnacle mats. **a** General view (coin 25 mm). **b** Cross section of pinnacle mat revealing the vertical structuring of the microbial community: from top to bottom, thin green layer, pink layer, black layer (for more information, see main text; coin 25 mm). **c** Reflected light photograph showing the association of diatoms (*arrows*) and filamentous cyanobacteria (scale 500 μm). **d** SEM image of a pinnacle with diatoms, most probably *Nitzschia* sp., and *Microcoleus chthonoplastes* bound by EPS (scale 2 μm). The filaments at the bottom and left show individual cells longer than wide, which is a typical attribute of *M. chthonoplastes*

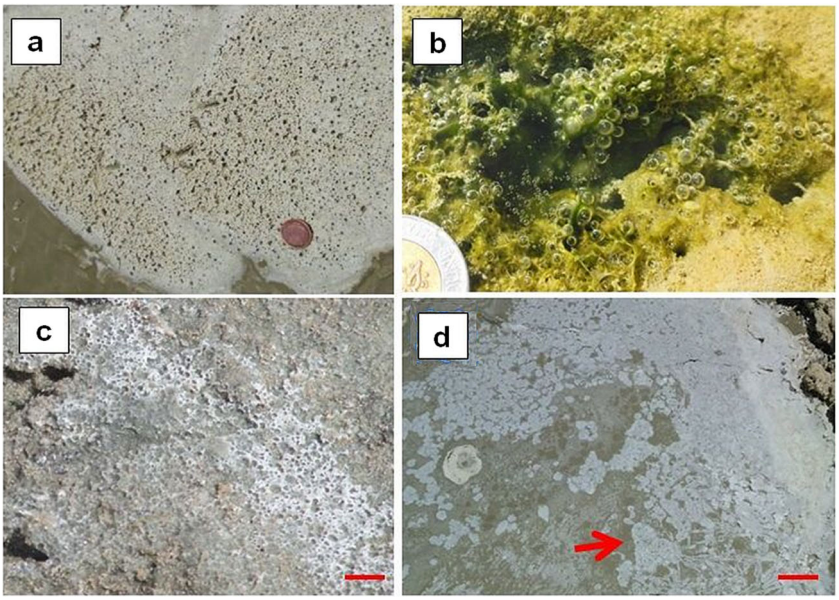

Fig. 8 **a** Bubbles solidified by salt crystallization, forming a sieve-like structure (coin 22 mm). **b** Freshly produced photosynthetic bubbles below a thin layer of water, emanating from the actively growing microbial community and stabilized by EPS forming nutrient-rich rims (coin 25 mm). **c** Partial salt crystallization infilling the spaces between bubbles (scale 20 mm). **d** Complete salt crystallization (rim-like). *Arrow* Partial crystallization around bubbles results in a solidified sieve structure. Scale 20 mm

like aggregates. The crystals are long and prismatic, varying in size from 10 to 20 mm and radiating from a common centre (Fig. 11b). Parts of the crusts often detach from the underlying substrate as small, circular or elongated sheets. Below the crusts, the organic matter content is high.

Petrographic analyses revealed the presence of idiomorphic euhedral crystals of trona with significant amounts of halite and argillites growing on the surface of microbial mats (Fig. 5d). The SEM images showed evidence of surface dissolution of halite clusters (Fig. 11c), associated with remnants of biofilms. Alveolar reniform thenardite occurs together with anhedral halite (Fig. 11d). Single crystals and clusters of randomly arranged, euhedral to subhedral crystals of thenardite are associated with acicular trona crystals (Fig. 11e). Individual thenardite crystal columns can be 10 μm long, and in places form patches.

Discussion and conclusions

In the El Beida Lake study area, the present findings demonstrate that low-gradient saline pools and adjoining flats are

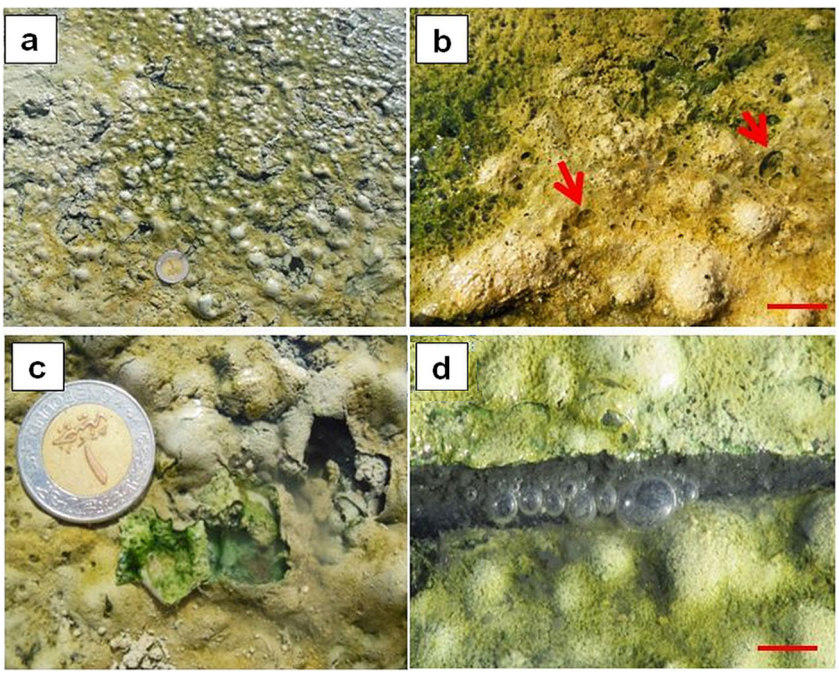

Fig. 9 Gas domes. **a** Freshly formed gas domes with rounded, intact surfaces (blisters; coin 25 mm). **b** Gas domes with bottom biofilm layer (scale 10 mm). **c** Close up of dome with collapsed surface and hollow interior (coin 25 mm). **d** Shallow trench in gas domes showing underlying organic-rich sediments associated with gas escape (scale 10 mm)

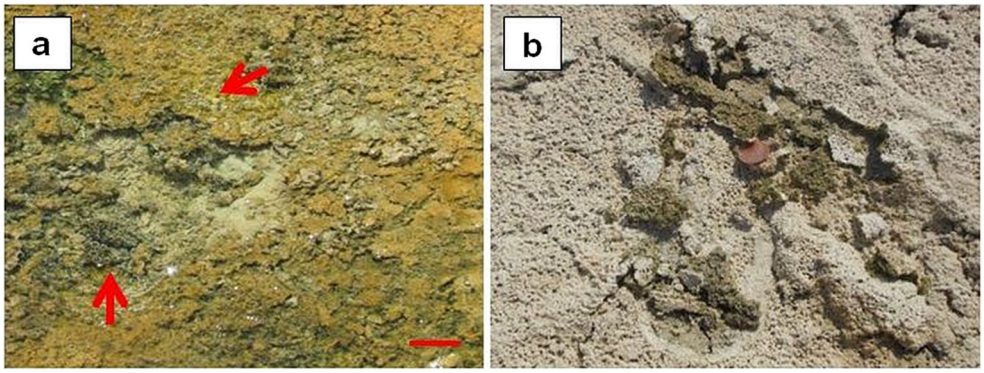

Fig. 10 **a** Irregularly shaped mat fragments, often with rounded to subrounded edges (scale 20 mm). *Arrows* Gas release. **b** Mat chips generated by wind-driven currents (coin 22 mm)

commonly colonized by cohesive microbial mats dominated by cyanobacteria associated with microbially induced sedimentary structures. By contrast, blocky salt crusts in marginal elevated areas are devoid of microbial mats. Goodall et al. (2000) reported similar salt crusts up to 1.5 m thick in Umm as-Samim in Oman, these being seldom subjected to surface flooding but receiving large amounts of brine from below. Smoot and Castens-Seidell (1994) recognized selective dissolution by rain in explaining the pitted appearance of high-relief salt crusts in the Saline Valley and Death Valley of the USA.

Knotty surfaces recorded in the higher parts of middle–lower supratidal flats and shallow parts of isolated pools in the present study area are consistent with the ability of filamentous cyanobacteria to grow vertically above the mat bottom (Buczynski and Chafetz 1993; Gerdes et al. 2000). When stabilized by EPS, initially soft and flexible tufts transform into rigid acmes (Fig. 3d, e). Gerdes (2007) provides a useful overview of environmental factors governing the formation of knotty surfaces, such as light, ionic composition of interstitial and surface water, and oxygen supply.

The mat cracks identified in the El Beida Lake study area differ from tepee structures resulting from salt crystallization pressure (Warren 1982). Evidence that the edges of cracks are usually rounded (Fig. 4b, c) is consistent with fracturing enabling the mat-forming microbes to overgrow the margins and evade the cracks (Gerdes et al. 2000). Overgrowth of margins under more moist conditions results in multilayered crack tapestries (Fig. 4c). The present findings also support those of Bose and Chafetz (2009) along the Texan coast of the USA—due to differential shrinkage between the top and bottom of a mat layer, the margins of mat crack polygons curl upwards, creating a bowl-like shape.

Wrinkle structures or Kinneyia are highly characteristic of Archean siliciclastic sediments (Noffke 2010), and are widespread in the present study area (Fig. 5a). Their formation

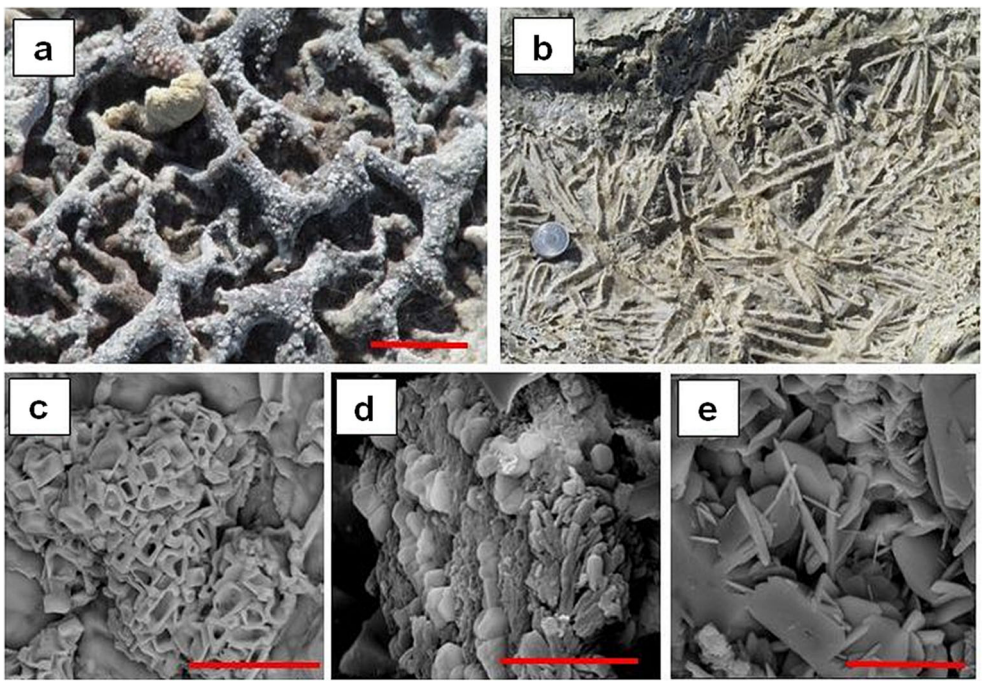

Fig. 11 Mineral precipitation. **a** Scattered, white halite crystals on the surface of microbial mats (scale 50 mm). **b** Aggregates of trona crystals radiating from a common centre (coin 20 mm). **c** SEM image of halite crystal aggregates with pitted surfaces (scale 20 μm). **d** Biofilm of alveolar reniform thenardite (lower right) together with anhedral halite crystals (scale 5 μm). **e** Thenardite and acicular trona crystals (scale 10 μm)

reflects the coherence of microbial mats, whereby less coherent mats tend to generate cylindrical rollup structures (Eriksson et al. 2000; Bose and Chafetz 2009). Patchy forms are strongly related to wind drift, rather than sedimentation processes in the El Beida Lake (Fig. 5b). Their formation is steered by the marked seasonal fluctuations in salinity and temperature characterizing this region. Indeed, wrinkle structures showed various degrees of lithification (Fig. 5b, c). The origin of wrinkle structures has received considerable attention in recent decades (for recent overview, see Noffke 2010). The findings of the present study are not inconsistent with hydrodynamics-induced effects explored in the laboratory study of Thomas et al. (2013) and by Cuadrado et al. (2014) in the Bahía Blanca Estuary of Argentina.

Reticulated surfaces in the low-lying shallow pools and associated feeder channels of the present study area reflect vertical growth of filamentous cyanobacteria above the mat surface (for overview, see Gerdes et al. 2000). In Shark Bay, Western Australia, Browne et al. (2000) interpreted reticulate mats dominated by *Lyngbya* sp. in terms of upward growth promoted by improved oxygenation. Experimental work by Shepard and Sumner (2010) has shown that undirected motility of filamentous cyanobacteria produces reticulate mats. Gerdes and Klenke (2003) observed that distinct microbial populations typify specific compartments of these surfaces, involving segregation amongst *Microcoleus chthonoplastes*, *Spirulina* sp. and coccoid *Synechococcus* sp. This aspect awaits further research in the El Beida Lake of Wadi El Natrun.

In the El Beida Lake study area, the results show that pinnacle distribution is overall random in pinnacle mats, one exception being their higher abundance around gas domes. Pinnacle height rarely exceeds 20 mm, contrasting with the findings of Park (1977) who reported pinnacles as much as 60 mm high along the Trucial Coast of the Persian Gulf. Flannery and Walter (2012) found that all known modern examples of pinnacle microbial mats are structurally dominated by filamentous cyanobacteria. Most pinnacles in the present study are associated with *M. chthonoplastes* and diatoms, probably *Nitzschia* sp. (Fig. 7c, d). Similarly, pinnacle mats of *M. chthonoplastes* and *Nitzschia* sp. occur in the Solar Lake, Red Sea (Krumbein and Cohen 1977). *M. chthonoplastes* is the key mat-forming cyanobacterium of, for example, saline lakes in Australia (Bauld 1986) and the Caballo Alba soda lake of Spain (Guerrero and de Wit 1992). Gerdes et al. (1994) highlighted the role of space competition between diatoms and cyanobacteria for favourable light conditions. Also, the spatial distribution of diatoms is strongly impacted by the upward migration of the O_2–H_2S chemocline at night (Jørgensen 1989; Gerdes et al. 1994). *M. chthonoplastes* uses the diatom valves as substrate, thereby promoting vertical pinnacle development.

In the formation of sieve-like structures identified in the study area (Fig. 8a), EPS-induced stabilization of bubbles would be an essential step (Eriksson et al. 2007; Bosak et al. 2010). Bose and Chafetz (2009) revealed that the slow rate of oxygen production by microbial mats greatly extends the persistence of bubbles in water, thereby facilitating salt precipitation around the bubbles before they escape (Fig. 8b–d). Crystallization progresses thermodynamically from the outside to the inside of the bubbles, forming sphere-like signatures (Fig. 8d).

Gas domes growing on mat surfaces in the study area (Fig. 9) are at least partly sourced in the decay of buried organic matter identified in deeper layers, as commonly reported from various world regions (see Noffke 2010). Other sources include photosynthetic activity, and gases trapped within intergranular spaces during sedimentation. Noffke et al. (2001) suggested that cohesive microbial mats inhibit gas escape, thereby promoting doming. Common gases encountered in such environments are long known to be CO_2, O_2, H_2S and methane (e.g. Stal et al. 1985; Giani et al. 1989). In the present case, the presence of O_2 was verified by using a flame that reignited close to the gas domes.

In the study area, mat-stabilized sediment surfaces would plausibly be detached and then further fragmented by strong currents driven by onshore winds, generating mat chips (Fig. 10). Locally, farm animals crossing the pools would further disturb the mats. The role of wind has been evoked also by, for example, Bouougri and Porada (2007) in their study of Tunisian tidal flats. In other world regions, additional factors involve mat cracking, jelly rolls, and subsurface gas (e.g. Gerdes et al. 2000; Gerdes 2007).

The present results revealed the occurrence of thenardite, trona and halite in the El Beida Lake study area (Fig. 11). In fact, Nakhla et al. (1985) documented that this lake contains the purest primary thenardite deposit worldwide, reaching 60% at some locations. Trona is associated with thenardite in most precipitates. In the geologic record, the presence of trona and other sodic carbonates in bedded evaporites deposited over the last 600–800 million years indicates a nonmarine brine source (Warren 2010). In the El Beida Lake, halite is the dominant mineral in summer, occurring in only small amounts in spring. Surface dissolution of halite can be associated with a former presence of cyanobacteria. Indeed, the interior of such halite crystals forms a moist microhabitat promoting the survival of microbial colonies, as well as protecting them against cosmic radiation (e.g. Wierzchos et al. 2006; Taher 2014b).

In the El Beida Lake, however, the surfaces containing salt minerals are highly dynamic, and would involve repeated dissolution and re-precipitation under strongly varying environmental conditions. These interpretations are consistent with the findings of Shortland (2004) and Shortland et al. (2011) at various sites in Wadi El Natrun. Evidently, complex interactions amongst surface hydrological cycles and diagenetic processes in the El Beida Lake may eventually obliterate MISS signatures either completely or at least partially. Such

challenges have been recognized also by Aref et al. (2014) for modern evaporitic coastal environments of Saudi Arabia and Egypt, and implicitly by Duane et al. (2015) for an exhumed Miocene inlier with mud volcanoes on a Persian Gulf sabkha.

MISS in the geologic record

Microbially induced sedimentary structures are known from various ancient environments (for recent overview, see Noffke et al. 2013). Observations of modes of formation of MISS in modern environments can serve for palaeoclimate and palaeoenvironmental reconstructions, particularly if MISS are identified in lithified rock (e.g. Cuadrado et al. 2014). In principle, MISS have good preservation potential in sedimentary rocks but only if associated with in situ mineral precipitation (e.g. Gerdes and Krumbein 1987; Schieber et al. 2007; Carmona et al. 2012; Taher 2014a). Archean and Proterozoic stromatolites are also generally thought to have been preserved via mineral precipitation.

Recent years have seen an increasing recognition of the relevance of modern MISS signatures in deciphering the geological record. For example, in their study of mat cracks on Tunisian tidal flats, Bouougri and Porada (2007) documented alternating mat growth and upturning of crack margins leading to complex structures along crack margins. Similarly, the present study reports evidence of mats with upward-curling margins in the El Beida Lake of Egypt (Fig. 4b, c). The identification of such complex structures in ancient laminated siliciclastic sediments would argue for the biogenicity of the deposits in an intertidal environment where constant/intermittent shrinkage and growth closely accompanied cyclic growth of mat–sediment doublets (Bouougri and Porada 2007). Likewise, the Lower Triassic Ormskirk Sandstone Formation in the Irish Sea Basin has been interpreted as reflecting both biogenic mat and salt crust growth on low-lying, occasionally flooded salt flats (Goodall et al. 2000). Moreover, mat cracks are exceptionally well preserved in the 2.9 Ga Pongola Supergroup of South Africa (Noffke et al. 2008).

The recognition of gas-related morphologies in the fossil record requires not only that bubbles form and attach to microbial mats but also that the mats be preserved by lithification (Bosak et al. 2010). In the present study, authigenic mineral precipitation within dense bubble-enclosing mats (Fig. 8a, c, d) would facilitate the preservation of gas bubbles as sieve-like structures that, in principle, may become distinct microstructures on ancient bedding surfaces. Bubbles in fossil microbialites are recognizable as near-circular cross sections enclosed by organic-rich laminae, such as those of Proterozoic conical stromatolites (Bosak et al. 2009).

Fossil gas domes with a central crater-like depression have been reported in fine-grained Mn sandstone of the Lower Pleistocene on the island of Milos, Greece, and interpreted to have formed in a littoral palaeoenvironment (Kilias 2011). Collapsed and non-collapsed domes may coexist on the same bed surface, as found in the present study (Fig. 9a, c) and discussed also by Noffke et al. (2013). Ruptured gas domes have been documented in the 1.6 Ga Chorhat Sandstone, Vindhyan Supergroup, India (Sarkar et al. 2006).

Wrinkle structures are an important tool for reconstructing palaeoenvironments and benthic palaeoecology in strata largely devoid of body and trace fossils (Calner and Eriksson 2012). They are common in Proterozoic to Palaeozoic rocks extending from intertidal to deep marine settings (e.g. Hagadorn and Bottjer 1999; Mata and Bottjer 2009; Calner and Eriksson 2012; Eriksson et al. 2012). Moreover, the Lower Arenigian (Ordovician) rocks of the Montagne Noire, France (Noffke 2000) represent a high-latitude, shallow marine environment along the northern margin of Gondwana. Wrinkle structures have been interpreted as fossil microbial mats comprising cyanobacterial communities. The mats are apparently of variable thickness, wrinkle structures in some cases being 'transparent' with underlying ripple marks visible on the surface (Fig. 5a in the present study), whereas they are 'non-transparent' in other cases where the original surface presents a smooth relief (Noffke 2000).

In conclusion, geomorphological zones in the alkaline hypersaline El Beida Lake of Wadi El Natrun in Egypt are an ideal environment for the growth of microbial mats associated with microbially induced sedimentary structures in a setting characterized by low sedimentation, lack of bioturbation, essentially no wave action, and protection by thick albeit patchy vegetation. The MISS identified are knotty surfaces, mat cracks, wrinkle structures, reticulate surfaces, pinnacle mats, sieve-like surfaces, gas domes and mat chips, associated with thenardite, trona and halite. Complex interactions between regional hydrological cycles and diagenetic processes imply low preservation potential. MISS signatures of such saline lakes can serve as key analogues for interpreting the geologic record.

Acknowledgements The authors gratefully acknowledge constructive reviews from Drs. N. Noffke and D. Cuadrado, as well as the journal editors. Sincere thanks are extended to Dr. G.J. Tassie (University of North Cornwall, UK) for English editing and critical reading, Dr. M. Abdel Moaty (Egyptian Geological Survey) for SEM analyses, and S. El Tayar (Cairo University) for field and laboratory assistance.

Conflict of interest The authors declare that they have no conflict of interest.

References

Abd El Ghani M, Hamdy R, Hamed A (2014) Aspects of vegetation and soil relationships around athalassohaline lakes of Wadi El-Natrun, Western Desert, Egypt. J Biol Earth Sci 4(1):B21–B35

Abd-el-Malek Y, Rizk SG (1963) Bacterial sulfate reduction and the development of alkalinity. III. Experiments under natural conditions in the Wadi Natrûn. J Appl Microbiol 26:20–26

Abu Khadra A (1973) Geological and sedimentological studies of Wadi El-Natrun district, Western Desert, Egypt. PhD Thesis, Cairo University, Egypt

Abu Zeid KA (1984) Contribution to the geology of Wadi El-Natrun area and its surroundings. MSc Thesis, Cairo University, Egypt

Aref MAM, Basyoni MH, Bachmann GH (2014) Microbial and physical sedimentary structures in modern evaporitic environments of Saudi Arabia and Egypt. Facies 60(2):371–388

Attia AKM, Hilmy ME, Bolous SN (1970) Mineralogy of the encrustation deposits of Wadi El-Natrun. Desert Inst Bull 2:301–325

Bauld J (1986) Benthic microbial communities of Australian saline lakes. In: de Deckker P, Williams WD (eds) Limnology in Australia. W. Junk, Boston, pp 95–111

Bosak T, Liang B, Sim MS, Petroff AP (2009) Morphological record of oxygenic photosynthesis in conical stromatolites. Proc Natl Acad Sci USA 106:10939–10943

Bosak T, Bush JWM, Flynn MR, Liang B, Ono S, Petroff AP, Sim MS (2010) Formation and stability of oxygen-rich bubbles that shape photosynthetic mats. Geobiology 8:45–55

Bose S, Chafetz HS (2009) Topographic control on distribution of modern microbially induced sedimentary structures (MISS): a case study from Texas coast. Sediment Geol 213:136–149

Bouougri EH, Porada H (2007) Complex structures associated with siliciclastic biolaminites. In: Schieber J, Bose PK, Eriksson PG, Banerjee S, Sarkar S, Altermann W, Catuneanu O (eds) Atlas of microbial mat features preserved within the siliciclastic rock record. Atlases in Geoscience, vol 2. Elsevier, Amsterdam, pp 111–115

Bouougri EH, Porada H, Reitner J, Gerdes G (2012) Introduction to the special issue "Signatures of microbes and microbial mats and the sedimentary record". Sediment Geol 263–264:1–5

Browne KM, Golubic S, Seong-Joo L (2000) Shallow marine microbial carbonate deposits. In: Riding RE, Awaramik SM (eds) Microbial sediments. Springer, Berlin, pp 233–249

Buczynski C, Chafetz HS (1993) Habit of bacterially induced precipitates of calcium carbonate: examples from laboratory experiments and recent sediments. In: Rezak R, Lavoie DL (eds) Carbonate microfacies. Springer, New York, pp 105–116

Calner M, Eriksson ME (2012) The record of microbially induced sedimentary structures (MISS) in the Swedish Paleozoic. In: Noffke N, Chafetz H (eds) Microbial mats in siliciclastic depositional systems through time. SEPM Spec Publ 101:29–36

Carmona NB, Ponce JJ, Wetzel A, Bournod CN, Cuadrado DG (2012) Microbially induced sedimentary structures in Neogene tidal flats from Argentina: paleoenvironmental, stratigraphic and taphonomic implications. Palaeogeogr Palaeoclimatol Palaeoecol 353–355:1–9

Cuadrado D, Perillo GME, Vitale AJ (2014) Modern microbial mats in siliciclastic tidal flats: evolution, structure and the role of hydrodynamics. Mar Geol 352:367–380

Decho AW (2000) Exopolymer microdomains as a structuring agent for heterogeneity within microbial biofilms. In: Riding R, Awramik SM (eds) Microbial sediments. Springer, Berlin, pp 9–15

Duane MJ, Reinink-Smith L, Eastoe C, Al-Mishwat AT (2015) Mud volcanoes and evaporite seismites in a tidal flat of northern Kuwait—implications for fluid flow in sabkhas of the Persian (Arabian) Gulf. Geo-Mar Lett 35:237–246. doi:10.1007/s00367-015-0403-9

El Hadidi MN (1993) Natural vegetation. In: Graig GM (ed) The agriculture of Egypt. Oxford University Press, London, pp 39–62

Eriksson PG, Simpson EL, Eriksson KA, Bumby AJ, Steyn GL, Sarkar S (2000) Muddy roll-up structures in siliciclastic interdune beds of the c. 1.8 Ga Waterberg Group, South Africa. Palaios 15:177–183

Eriksson PG, Schieber J, Bouougri E, Gerdes G, Porada H, Banerjee S, Bose PK, Sarkar S (2007) Classification of structures left by microbial mats in their host sediments. In: Schieber J, Bose PK, Eriksson PG, Banerjee S, Sarkar S, Altermann W, Catuneanu O (eds) Atlas of microbial mat features preserved within the clastic rock record. Elsevier, Amsterdam, pp 39–52

Eriksson PG, Bartman R, Catuneanu O, Mazumder R, Lenhardt N (2012) A case study of microbial mat-related features in coastal epeiric sandstones from the Paleoproterozoic Pretoria Group (Transvaal Supergroup, Kaapvaal craton, South Africa): the effect of preservation (reflecting sequence stratigraphic models) on the relationship between mat features and inferred paleoenvironment. Sediment Geol 263–264:67–75

Flannery DT, Walter MR (2012) Archean tufted microbial mats and the Great Oxidation Event: new insights into an ancient problem. Aust J Earth Sci 59(1). doi:10.1080/08120099.2011.607849

Gerdes G (2007) Structures left by modern microbial mats in their host sediment. In: Schieber J, Bose PK, Eriksson PG, Banerjee S, Sarkar S, Altermann W, Catuneanu O (eds) Atlas of microbial mat features preserved within the siliciclastic rock record. Elsevier, Amsterdam, pp 5–38

Gerdes G (2010) What are microbial mats? In: Seckbach J, Oren A (eds) Microbial mats. Modern and ancient microorganisms in stratified systems. Springer, Dordrecht, pp 5–28

Gerdes G, Klenke T (2003) Geologische Bedeutung ökologischer Zeitr ume in biogener Schichtung (Mikrobenmatten, potentielle Stromatolithe). Mitt Ges Geol Bergbaustud Öster 46:35–49

Gerdes G, Krumbein WE (1987) Biolaminated deposits. Lecture Notes in Earth Sciences, vol 9. Springer, Berlin

Gerdes G, Krumbein WE, Reineck HE (1994) Microbial mats as architects of sedimentary surface structures. In: Krumbein WE, Stal LJ, Paterson DM (eds) Biostabilization of sediments. BIS, Oldenburg, pp 165–182

Gerdes G, Klenke T, Noffke N (2000) Microbial signatures in peritidal siliciclastic sediments: a catalogue. Sedimentology 47:279–308

Giani D, Seeler J, Giani L, Krumbein WE (1989) Microbial mats and physicochemistry in a saltern in the Bretagne (France) and in a laboratory scale saltern model. FEMS Microb Ecol 62:151–162

Goodall M, North CP, Glennie KW (2000) Surface and subsurface sedimentary structures produced by salt crusts. Sedimentology 47:99–118

Grünke S, Lichtschlag A, de Beer D, Felden J, Salman V, Ramette A, Schulz-Vogt HN, Boetius A (2012) Mats of psychrophilic thiotrophic bacteria associated with cold seeps of the Barents Sea. Biogeosciences 9:2947–2960

Guerrero MC, de Wit R (1992) Microbial mats in the inland saline lakes of Spain. Limnetica 8:197–204

Hagadorn JW, Bottjer DJ (1999) Restriction of a late Neoproterozoic biotope: suspect microbial structures and trace fossils at the Vendian–Cambrian transition. In: Hagadorn JW, Pflüger F, Bottjer DJ (eds) Unexplored microbial worlds. Palaios 14:73–85

Hagadorn JW, McDowell C (2012) Microbial influence on erosion, grain transport and bedform genesis in sandy substrates under unidirectional flow. Sedimentology 59:795–808

Jeanthon C (2000) Molecular ecology of hydrothermal vent microbial communities. Antonie van Leeuwenhoek 77:117–133

Jørgensen BB (1989) Light penetration, absorption and action spectra in cyanobacterial mats. In: Cohen Y, Rosenberg E (eds) Microbial mats. Physiological ecology of benthic microbial communities. ASM, Washington, DC, pp 123–137

Kilias S (2011) Microbial mat-related structures in the Quaternary Cape Vani manganese oxide (-barite) deposit, NW Milos Island, Greece. In: Noffke N, Chafetz H (eds) Microbial mats in siliciclastic depositional systems through time. SEPM Spec Publ 101:97–110

Knoll A, Canfield D, Konhauser K (2012) Fundamentals of geobiology. Wiley-Blackwell, London

Krumbein WE, Cohen Y (1977) Primary production, mat formation and lithification: contribution of oxygenic and facultative anoxygenic

cyanobacteria. In: Flügel E (ed) Fossil algae. Springer, Berlin, pp 37–56

Mata SA, Bottjer DJ (2009) The paleoenvironmental distribution of Phanerozoic wrinkle structures. Earth-Sci Rev 96:181–195

Mesbah MN, Abou-El-Ela SH, Wiegel J (2007) Novel and unexpected prokaryotic diversity in water and sediments of the alkaline, hypersaline lakes of the Wadi An Natrun, Egypt. Microb Ecol 54:598–617

Nakhla FM, Saleh SA, Gad NL (1985) Mineralogy, chemistry and paragenesis of the thenardite (Na_2SO_4). In: Applied mineralogy. Metallurgical Society, AIME, New York, pp 1001–1013

Noffke N (1998) Multidirected ripple marks rising from biological and sedimentological processes in modern lower supratidal deposits (Mellum Island, southern North Sea). Geology 26:879–882

Noffke N (2000) Extensive microbial mats and their influences on the erosional and depositional dynamics of a siliciclastic cold water environment (Lower Arenigian, Montagne Noire, France). Sediment Geol 136:207–215

Noffke N (2010) Microbial mats in sandy deposits from the Archean era to today. Springer, Berlin

Noffke N (2015) Ancient sedimentary structures in the <3.7 Ga Gillespie Lake Members, Mars that resemble macroscopic morphology, spatial associations, and temporal succession in terrestrial microbialites. Astrobiology 15(2):169–192

Noffke N, Krumbein WE (1999) A quantitative approach to sedimentary surface structures controlled by the interplay of microbial colonization and physical dynamics. Sedimentology 46:417–426

Noffke N, Gerdes G, Klenke T, Krumbein WE (1997) A microscopic sedimentary succession indicating the presence of microbial mats in siliciclastic tidal flats. Sediment Geol 110:1–6

Noffke N, Gerdes G, Klenke T, Krumbein WE (2001) Microbially induced sedimentary structures—A new category within the classification of primary sedimentary structures. J Sediment Res 71:649–656

Noffke N, Beukes N, Hazen R, Swift D (2008) An actualistic perspective into Archean worlds – (cyano-)bacterially induced sedimentary structures in the siliciclastic Nhlazatse Section, 2.9 Ga Pongola Supergroup, South Africa. Geobiology 6:5–20

Noffke N, Decho AW, Stoodley P (2013) Slime through time: the fossil record of prokaryote evolution. Palaios 28:1–5

Park K (1977) The preservation potential of some recent stromatolites. Sedimentology 24:485–506

Pavlov M (1962) Preliminary report on the ground water beneath the Wadi El-Natrun and adjacent areas. Report to General Desert Development Organization of U.A.R. Desert Institute, Cairo

Phillip G, Barakat MG, Abu Khadrah A (1975) Stratigraphy and mechanical analysis of Neogene sediments in Wadi El-Natrun area, Egypt. Faculty of Science, Cairo University, Bull no 48

Saleh AH (2004) Sedimentological and evaluation studies of the Pliocene clays and their ability in industrial application in and around Wadi-El Natrun, Western Desert, Egypt. MSc Thesis, Menofiya University, Egypt

Sarkar S, Banerjee S, Samanta P, Jeevankumar S (2006) Microbial mat-induced sedimentary structures in siliciclastic sediments: examples from the 1.6 Ga Chorhat Sandstone, Vindhyan Supergroup, M.P., India. J Earth Syst Sci 115(1):49–60

Schieber J, Bose PK, Eriksson PG, Sarkar S (2007) Palaeogeography of microbial mats in terrigenous clastics—environmental distribution of associated sedimentary features and the role of geologic time. In: Schieber J, Bose PK, Eriksson PG, Banerjee S, Sarkar S, Altermann W, Catuneanu O (eds) Atlas of microbial mat features preserved within the siliciclastic rock record, vol 2, Atlases in Geoscience. Elsevier, Amsterdam, pp 267–275

Shata A, El-Fayoumi IF (1967) Geomorphological and morphopedological aspects of the region west of the Nile Delta with special reference to Wadi El-Natrun area. Bull Inst Désert Egypte 12(1):1–38

Shepard RN, Sumner DY (2010) Undirected motility of filamentous cyanobacteria produces reticulate mats. Geobiology 8(3):179–190

Shortland AJ (2004) Evaporites of the Wadi Natrun: seasonal and annual variation and its implication for ancient exploitation. Archaeometry 46(4):497–516

Shortland AJ, Degryse P, Walton M, Geer M, Lauwers V, Salou L (2011) The evaporitic deposits of Lake Fazda (Wadi Natrun, Egypt) and their use in Roman glass production. Archaeometry 53(5):916–929

Smoot JP, Castens-Seidell B (1994) Sedimentary features produced by efflorescent salt crusts, Saline Valley and Death Valley, California. In: Renaut RW, Last WM (eds) Sedimentology and geochemistry of modern and ancient lakes. SEPM Spec Publ 50:73–90

Stal LJ, Gemerden H, Krumbein WE (1985) Structure and development of benthic marine microbial mats. FEMS Microb Ecol 31:111–125

Sturchio N, Sultan M, El-Alfy Z, Taher AG, El-Maghraby A, El-Anabaawy M (1998) Geochemistry and origin of ground water in the newly reclaimed agricultural lands, western Nile Delta, Egypt: preliminary isotopic results. In: Proc 4th Int Conf Geology of the Arab World. Cairo University, Egypt

Taher AG (1999) Inland saline lakes of Wadi El Natrun depression, Egypt. Int J Salt Lake Res 8:149–169

Taher AG (2014a) Formation and calcification of modern gypsum-dominated stromatolites, EMISAL, Fayium, Egypt. Facies 60: 721–735

Taher AG (2014b) Microbially induced sedimentary structures in evaporite–siliciclastic sediments of Ras Gemsa sabkha, Red Sea Coast, Egypt. J Adv Res 5:577–586

Taher AG, Abdel Motelib A (2014) Microbial stabilization of sediments in a recent Salina, Lake Aghormi, Siwa Oasis, Egypt. Facies 60:45–52

Taher AG, Soliman A (1999) Heavy metals concentrations in surficial sediments from Wadi El-Natrun saline lakes, Egypt. Int J Salt Lake Res 8:75–92

Taher AG, Abdel Wahab S, Krumbein WE, Philip G, Wali A (1994) On heavy metal concentrations and biogenic enrichment in microbial mats. Miner Deposita 29:427–429

Thomas K, Herminghaus S, Porada H, Goehring L (2013) Formation of Kinneyia via shear-induced instabilities in microbial mats. Philos Trans R Soc A 371:20120362. doi:10.1098/rsta.2012.0362

Warren JK (1982) The hydrogeological significance of Holocene tepees, stromatolites, and boxwork limestones in coastal salinas in South Australia. J Sediment Petrol 52:1171–1201

Warren JK (2010) Evaporites through time: tectonic, climatic and eustatic controls in marine and nonmarine deposits. Earth-Sci Rev 98:217–268

Wierzchos J, Ascaso C, McKay CP (2006) Endolithic cyanobacteria in halite rocks from the hyperarid core of the Atacama Desert. Astrobiology 6(3):415–422

Wrede C, Kokoschka S, Dreier A, Heller C, Reitner J, Hoppert M (2013) Deposition of biogenic iron minerals in a methane oxidizing microbial mat. Archaea, 102972. doi:10.1155/2013/102972

Yallop ML, de Winder B, Paterson DM, Stal LJ (1994) Comparative structure, primary production and biogenic stabilization of cohesive and non-cohesive marine sediments inhabited by microphytobenthos. Estuar Coastal Shelf Sci 39:565–582